Supporting Information

For

Enhancing Metabolite Coverage in MALDI-MSI using Laser Post-Ionisation (MALDI-2).

J.C.McKinnon,[a] H.H.Milioli,[b,c,d] C.A.Purcell,[b,c,d] C.L.Chaffer,[b,c,d] B.Wadie,[e] T.Alexandrov,[e] T.W.Mitchell[f] and S.R.Ellis*[a]

[a] Molecular Horizons and School of Chemistry and Molecular Bioscience, University of Wollongong, Northfields Ave, Wollongong, NSW 2522, Australia.

[b] Garvan Institute of Medical Research, Darlinghurst, NSW, Australia

[c] St. Vincent's Clinical School, UNSW Medicine, UNSW Sydney, NSW, Australia

[d] The Kinghorn Cancer Centre, Darlinghurst, NSW, Australia

[e] Structural and Computational Biology Unit, European Molecular Biology Laboratory (EMBL), Heidelberg, Germany.

[f] Molecular Horizons and School of Medical, Indigenous and Health Science, University of Wollongong, Northfields Ave, Wollongong, NSW 2522, Australia

To whom correspondence should be addressed:

sellis@uow.edu.au

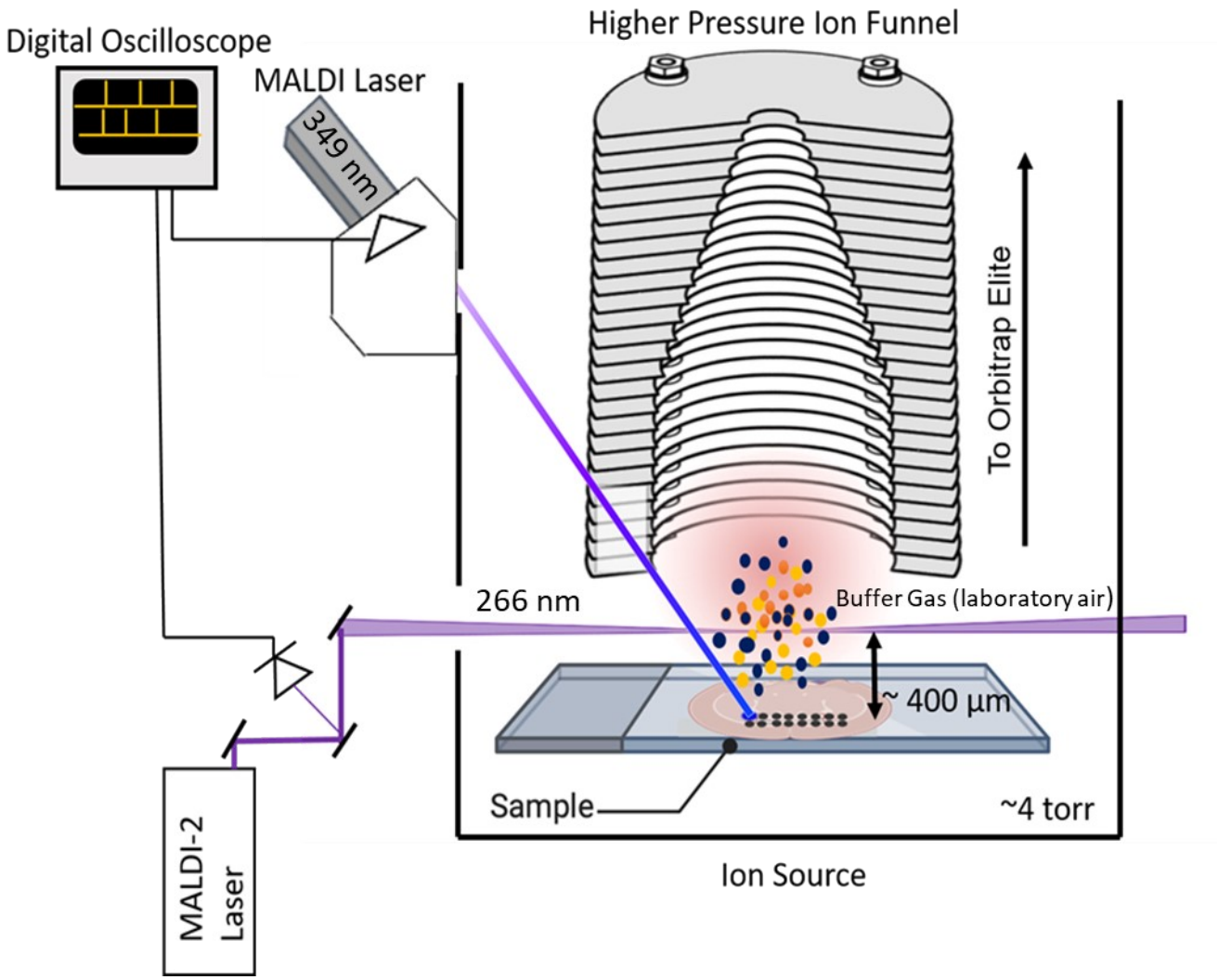

Figure S1: Schematic of experimental set-up.

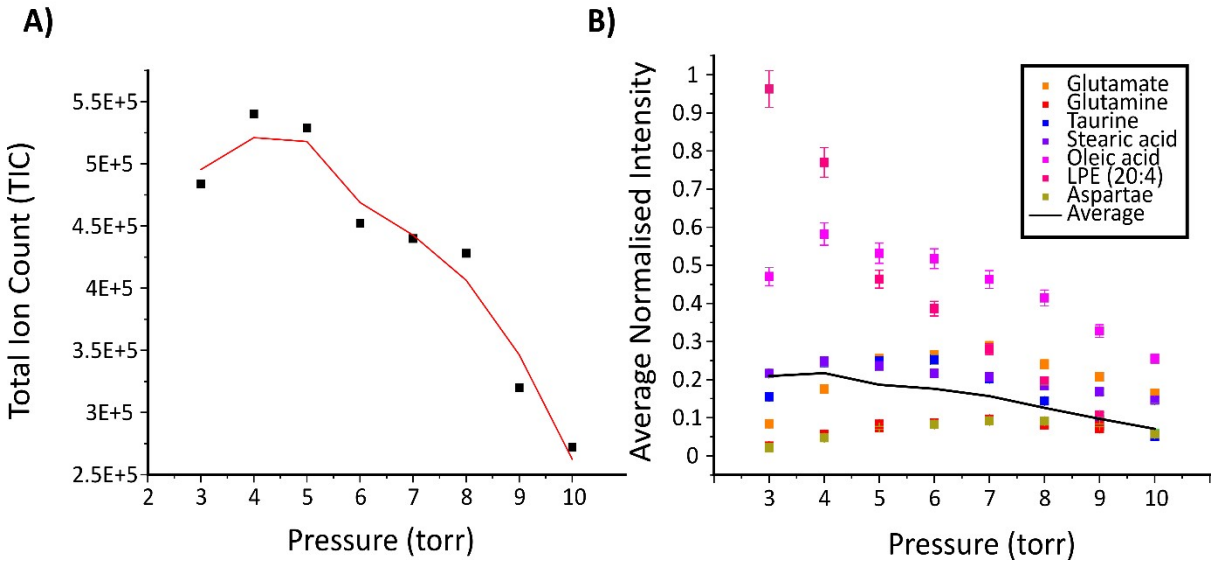

Figure S2: **A)** the influence of ion source pressure on the total ion count (TIC) of successive line scans across liver homogenate tissue acquired in the negative ion mode at a 60 µm x 60 µm pixel size. **B)** the derived ion intensities of selected tentatively identified analytes from pressure optimisation experiments (n=3) as detailed in the methods section of the main text. Error bars display the ±1 standard deviation for each data point (n=3 measurements).

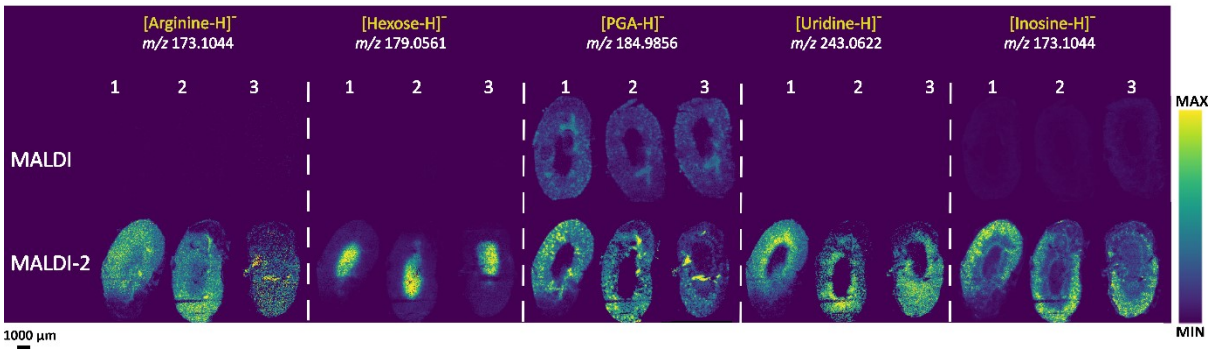

Figure S3: Metabolite images across (n = 3) technical replicates of the species shown in Fig.2c-g of main text. The resulting images are displayed with no normalisation applied so as to directly compare changes in absolute signal intensity between each method. Hotspot removal (high quantile value 99%) was applied for visualisation of ion images.

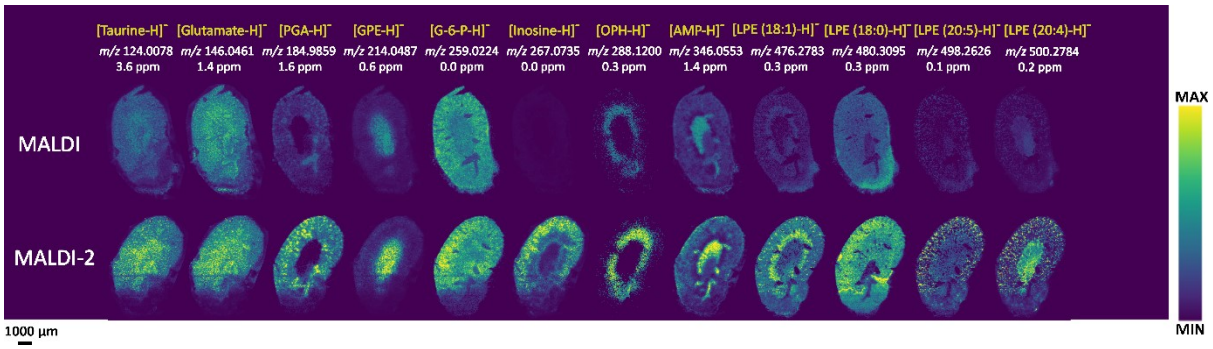

Figure S4: Selected ion images generated via MALDI (M) and MALDI-2 (M-2) of endogenous metabolite species detected from adjacent mouse kidney tissue with a pixel size of 60 µm x 60 µm. The resulting images are displayed with no normalisation applied so as to directly compare changes in absolute signal intensity between each method. Hotspot removal (high quantile value 99%) was applied for visualisation of ion images.

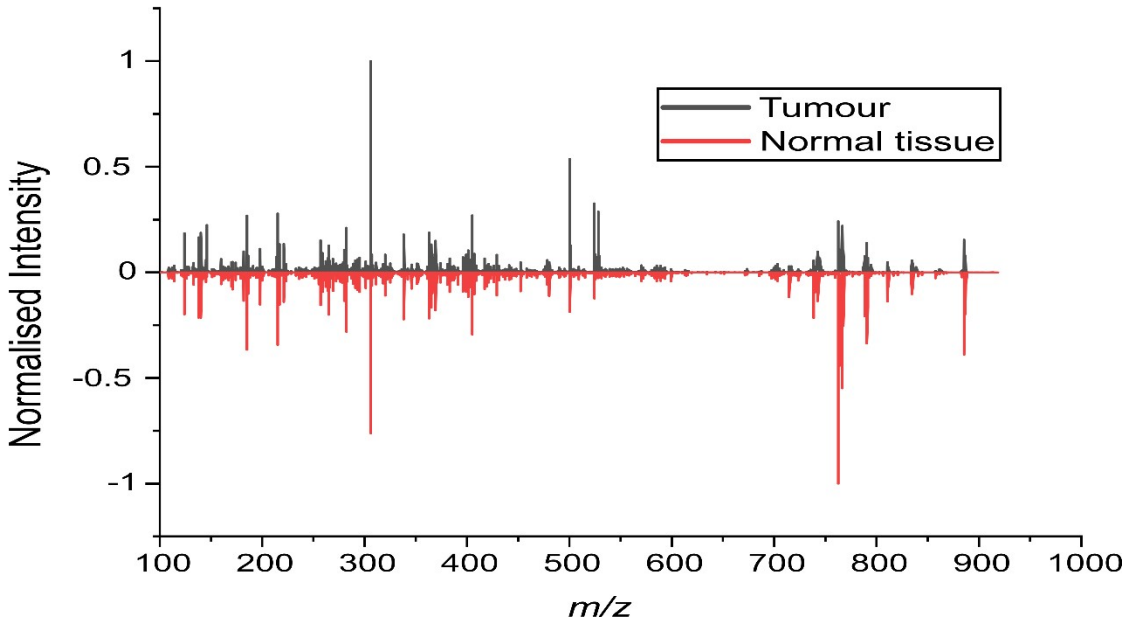

Figure S5: Averaged MALDI-2-MSI on-tissue spectra from the tumour and normal liver tissue defined regions for data shown in Figure 3.

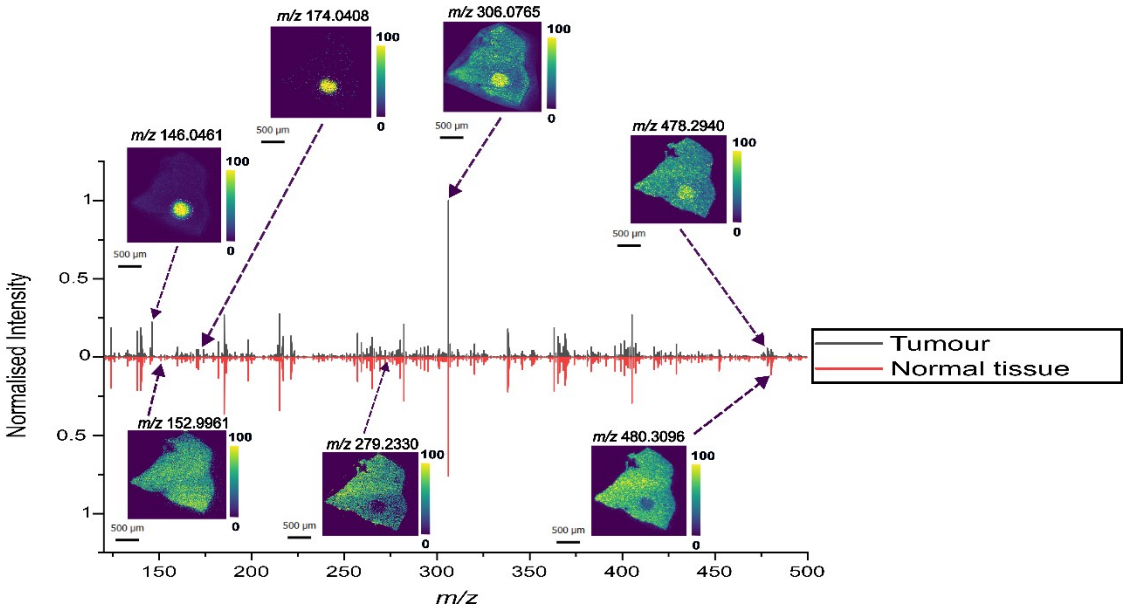

Figure S6: Enlarged *m/z* 100-500 range from the MALDI-2 derived cancer dataset shown in Figure 3. Averaged normalised spectrum from tumour region is shown as the black trace, and the surrounding tissue in the red trace. Ion images of selected m/z values are also provided. Ion images are visualised following total-ion current normalisation and hotspot removal (high quantile value 99%).

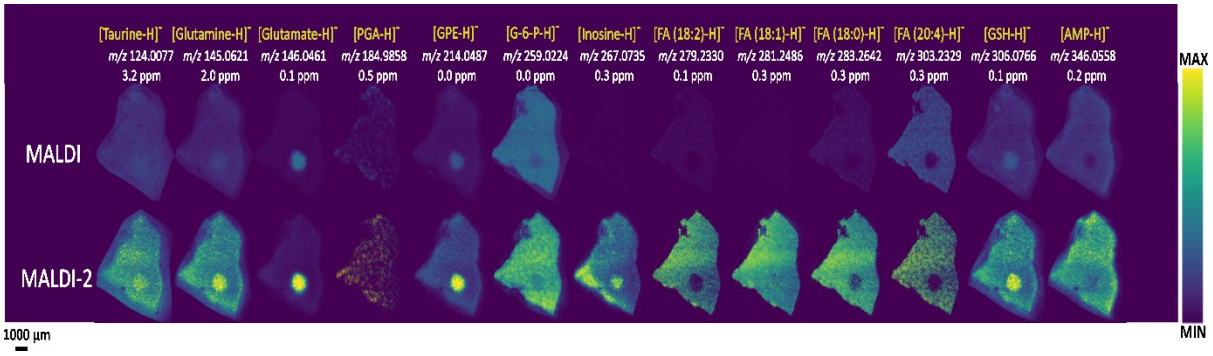

Figure S7: Selected ion images generated via MALDI (M) and MALDI-2 (M-2) of endogenous metabolite species detected from adjacent mouse kidney tissue with a pixel size of 60 µm x 60 µm. The resulting images are displayed with no normalisation applied so as to directly compare changes in absolute signal intensity between each method.

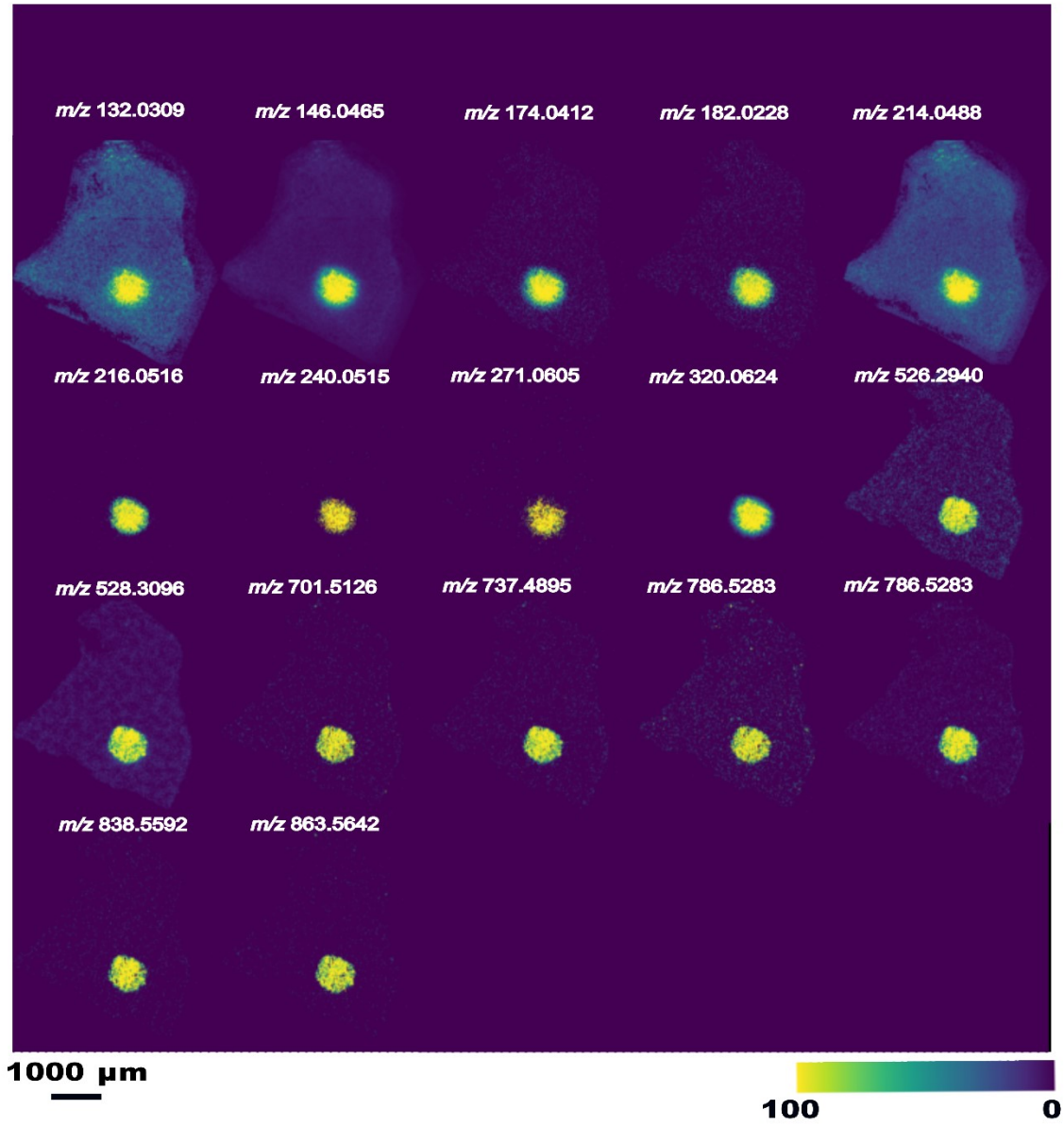

Figure S8: Ion images for m/z values which co-localise to the tumour tissue region generated using conventional MALDI-MSI from an adjacent tissue section to that shown in Figure 3. All images are referenced to the tumour region defined on the H&E stained tissue following co-registration with the MSI data and have Pearson correlation coefficients ≥0.6 with the tumour region. All images are generated using total ion count normalisation and hotspot removal (high quantile value 99%). Hotspot removal (high quantile value 99%) was applied for visualisation of ion images.

Table S1: Summary of laser parameters for both MALDI and MALDI-2 approaches. Note primary laser pulse energy is the pulse energy after passing through an external attenuator.

	Primary laser freq. (*Hz*)	**Primary laser diode current** (Amps)	**Primary laser pulse energy** (μJ)	**PI laser freq.** (*Hz*)	**PI laser pulse energy** (μJ)
MALDI	300	1.8	1.44	-	-
MALDI-2	300	1.8	1.44	300	600

Table S2: Table of 34 unique annotations from Figure 3 of main text provided as their sum elemental formula.

Elemental Formula	**Adduct**	***m/z***
MgCl2	[M+Cl]-	128.8921
C4H7NO4	[M-H]-	132.0302
H3O4P	[M+Cl]-	132.9463
CaCl2	[M+Cl]-	144.8697
C6H8O5	[M-H]-	159.0299
C13H6	$[M-H]^-$	161.0396
C11H8N2	$[M-H]^-$	167.0614
C2H8NO4P	[M+Cl]-	175.9885
H4O7P2	[M-H]-	176.9359
C6H8O7	[M-H]-	191.0197
C6H10O5	[M+Cl]-	197.0222
C5H13O7P	[M-H]-	215.0326
C16H12NO3	$[M-H]^-$	265.0744
C14H20O6	$[M-H]^-$	283.1187
C15H13ClO6	$[M-H]^-$	323.0328
C18H28N2O4	$[M-H]^-$	335.1976
C23H30O4	$[M-H]^-$	369.2071
C25H35NO4	[M-H]-	412.2493
C24H30O4	[M+Cl]-	417.1838
C23H30O5	$[M-H]^-$	421.1787
C23H29ClO4	$[M+Cl]^-$	439.1448
C23H35NO6S	[M-H]-	452.2112
C26H26O9	[M-H]-	481.1504
C24H40N5O8	[M-H]-	525.2804
C33H35N5O5	[M-H]-	580.2565
C21H39N7O12	$[M-H]^-$	580.2584
C33H37N5O5	[M-H]-	582.2722
C32H45NO9	[M-H]-	586.3021
C8H8O3	[M-H]-, [M+Cl]-	151.0400, 187.0167
C6H14N4O2	[M-H]-, [M+Cl]-	173.1044, 209.0810
C12H14N2	[M-H]-, [M+Cl]-	185.1084, 221.0851
C23H24O4	[M-H]-, [M+Cl]-	363.1601, 399.1368
C23H31ClO4	[M-H]-, [M+Cl]-	405.1838, 441.1604
C25H40N2O6S	[M-H]-, [M+Cl]-	495.2534, 531.2301

Table S3*:* Table of tentative metabolite annotations for species discussed in the main text.

Elemental Formula	Adduct	*Theoretical m/z*	Observed *m/z*	Name	*m/z* error (ppm)
C2H7NO3S	M-H	124.0073	124.0078	Taurine	3.6
C5H10N2O3	M-H	145.0619	145.0618	Glutamine	-0.7
C5H9NO4	M-H	146.0459	146.0461	Glutamate	1.4
C6H14N4O2	M-H	173.10436	173.1047	Arginine	1.7
C6H9NO5	M-H	174.0408	174.0406	*N*-acetyl-aspartic acid	-1.1
C2H8NO4PCl	M+Cl	175.9885	175.9886	Phosphoethanolamine	0.6
C6H12O6	M-H	179.0561	179.0565	Hexose	2.2
C5H9NO4Cl	M+Cl	182.0226	182.0227	Glutamate	0.5
C3H7O7P	M-H	184.9856	184.9859	2-Phosphoglyceric acid	1.6
C5H14NO6P	M-H	214.0486	214.0487	glycerophosphoethanolamine	0.6
C6H12O6Cl	M+Cl	215.0328	215.0332	Hexose	1.9
C9H12N2O6	M-H	243.0622	243.0621	Uridine	-0.4
C6H13O9P	M-H	259.0224	259.0224	Glucose-6-phosphate	0.0
C10H12N4O5	M-H	267.0735	267.0735	Inosine	0.0
C18H32O2	M-H	279.2329	279.2330	FA 18:2	0.4
C10H17N3O6S	M-H	306.0765	306.0765	Glutathione	0.0
C10H14N5O7P	M-H	346.0558	346.0553	Adenosine monophosphate	-1.4
C23H46NO7P	M-H	478.2939	478.294	LPE (18:1)	0.2
C23H48NO7P	M-H	480.3095	480.3097	LPE (18:0)	0.3
C25H44NO7P	M-H	500.2783	500.2784	LPE (20:4)	0.2
C27H46NO7P	M-H	526.2939	526.2940	LPE (22:5)	0.2
C27H48NO7P	M-H	528.3095	528.3097	LPE (22:4)	0.4
C27H50NO7P	M-H	530.3252	530.3253	LPE(22:3)	0.2
C29H50NO7P	M-H	554.3252	554.3256	LPE(24:5)	0.7
C29H47NO7	M+Cl	556.3047	556.3045	Deoxycholylglutamic acid	-0.4
C39H75O8P	M-H	701.5216	701.5218	PA(36:1)	0.3
C41H80NO8P	M-H	744.5548	744.5554	PE(36:1)	0.8
C40H76NO10P	M-H	760.5134	760.5132	PS(34:1)	-0.3
C42H78NO10P	M-H	786.5290	786.5286	PS(36:2)	-0.5
C42H80NO10P	M-H	788.5447	788.5440	PS(36:1)	-0.9
C45H80NO8P	M-H	792.5544	792.5546	PE(40:5)	0.3
C46H81NO10P	M-H	838.5604	838.5588	PS(40:4)	-1.9
C45H84O13P	M-H	863.5655	863.5647	PI(36:1)	-0.9

FA = Fatty acid

LPE – Lysophosphatidylethanolamine

PA – Phosphatidic acid

PE – Phosphatidylethanolamine

PS – Phosphatidylserine

PI - Phosphatidylinositol

** The presence of analyte isomers cannot be discounted, with putative identifications provided on the basis of high-resolution accurate mass matching to metabolite databases.